The Journal of Experimental Biology 211, 1463-1474
Published by The Company of Biologists 2008
doi:10.1242/jeb.017160

Mechanical specialization of the obliquely striated circular mantle muscle fibres of the long-finned squid *Doryteuthis pealeii*

Joseph T. Thompson[1,*], John A. Szczepanski[2] and Joshua Brody[2]

[1]Department of Biology, Franklin & Marshall College, PO Box 3003, Lancaster, PA 17604-3003, USA and [2]Department of Biology, St Joseph's University, 5600 City Avenue, Philadelphia, PA 19131, USA

*Author for correspondence (e-mail: joseph.thompson@fandm.edu)

Accepted 7 March 2008

SUMMARY

The centrally located, mitochondria-poor (CMP) and superficially located, mitochondria-rich (SMR) circular muscle fibres in the mantles of some squids provide one of the few known examples of specialization in an obliquely striated muscle. Little is known of the mechanical properties or of the mechanisms and performance consequences of specialization in these fibres. We combined morphological and physiological approaches to study specialization in the SMR and CMP fibres of the long-finned squid *Doryteuthis pealeii*. The mean thick filament length was 3.12±0.56 μm and 1.78±0.27 μm for the SMR and CMP fibres, respectively. The cross-sectional areas of the whole fibre and the core of mitochondria were significantly higher in the SMR fibres, but the area occupied by the myofilaments did not differ between the two fibre types. The area of sarcoplasmic reticulum visible in cross sections was significantly higher in CMP fibres than in SMR fibres. In live bundles of muscle fibres partially isolated from the mantle, mean peak isometric stress during tetanus was significantly greater in SMR [335 mN mm^{-2} physiological cross section (pcs)] than in CMP (216 mN mm^{-2} pcs) fibres. SMR fibres had a lower average twitch:tetanus ratio (SMR=0.073; CMP=0.18) and a twofold lower unloaded maximum shortening velocity at 20°C (SMR=2.4 L_0 s^{-1}; CMP=5.1 L_0 s^{-1}), where L_0 was the preparation length that yielded the highest tetanic force. The structural differences in the two muscle fibre types play a primary role in determining their mechanical properties, and the significant differences in mechanical properties indicate that squid have two muscle gears. A simple model of the mantle shows that a gradient of strain and strain rate exists across the mantle wall, with fibres adjacent to the outer edge of the mantle experiencing 1.3- to 1.4-fold lower strain and strain rate than fibres adjacent to the inner edge of the mantle. The model also predicts that the CMP fibres generate virtually no power for slow jetting while the SMR fibres are too slow to generate power for the escape jets. The transmural differences in strain and strain rate predicted by the model apply to any cylindrical animal that has circumferentially oriented muscle fibres and an internal body cavity.

Key words: cephalopod, obliquely striated muscle, circular muscles, thick filaments, mechanical properties, kinematics.

INTRODUCTION

Obliquely striated muscles, which have dense bodies (i.e. Z-elements) aligned at an oblique angle to the long axis of the cell, have been reported in members of at least eleven different invertebrate phyla: Annelida (e.g. Rosenbluth, 1968), Brachiopoda (Kuga and Matsuno, 1988), Bryozoa (Bouligand, 1966), Echinodermata (Carnevali et al., 1986), Mollusca (e.g. Kawaguti and Ikemoto, 1957; Matsuno and Kuga, 1989), Nematoda (e.g. Rosenbluth, 1965), Nemertea (Norenburg and Roe, 1997), Platyhelminthes (MacRae, 1965; Ward et al., 1986), Rotifera (Bouligand, 1966), Sipunculida (DeEguileor and Valvassori, 1977) and Urochordata (Bone and Ryan, 1974). Despite the ubiquity of obliquely striated muscles, their specialization has received relatively little attention. Two different fibre types have been reported for the longitudinal muscles of leeches (Rowlerson and Blackshaw, 1991), earthworms (D'Haese and Carlhoff, 1987), and the mantle and fins of some cephalopods (Bone et al., 1981; Mommsen et al., 1981; Kier, 1989), but both the mechanisms and performance consequences of specialization are virtually unknown.

Mantle muscle specialization

The mantle of squids is a conical muscular sac that encloses the organs and the mantle cavity. Its functions include providing mechanical support for the fins and power for respiratory ventilation movements and jet locomotion. The muscles of the mantle are arranged primarily in two orientations (Marceau, 1905; Williams, 1909; Young, 1938): circumferentially (the circular muscles) and radially (the radial muscles; Fig. 1). Contraction of the circular muscles drives water out of the mantle cavity *via* the funnel while contraction of the radial muscles helps to refill the mantle cavity with water at the end of the power stroke (Young, 1938). Many squid species possess two types of circular muscle cells: centrally located, mitochondria-poor (CMP) fibres and superficially located, mitochondria-rich (SMR) fibres (Figs 1, 2) (Bone et al., 1981; Mommsen et al., 1981) [terminology from Preuss et al. (Preuss et al., 1997)]. Both fibre types are obliquely striated (Marceau, 1905; Hanson and Lowy, 1957).

The SMR circular muscle fibres are hypothesized to provide power for ventilation of the mantle cavity and prolonged, slow-speed jetting (Bone et al., 1981; Mommsen et al., 1981; Bartol, 2001a). Conversely, the CMP circular muscle fibres are hypothesized to provide power for more vigorous and rapid jets, including escape jets (Bone et al., 1981; Mommsen et al., 1981; Gosline et al., 1983; Bartol, 2001a). The hypothesized functions of the SMR and CMP circular muscle fibres are based on several lines of evidence. (1)

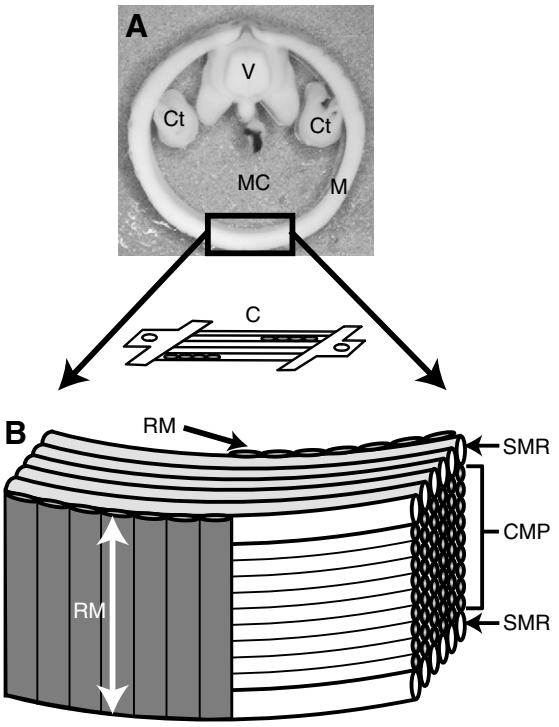

Fig. 1. Mantle morphology. (A) Photograph of a cross section of the formalin-fixed mantle of a juvenile *Doryteuthis pealeii*. The section was taken approximately from the midpoint along the length of the mantle. The diameter of the mantle is about 25 mm. Ctenidia (Ct), mantle (M), mantle cavity (MC), and viscera (V). (B) A schematic illustrating only the mantle muscles. The circular muscles compose the majority of the mantle musculature but regularly spaced bands of radial muscle fibres (RM) are also present. There are two types of circular muscles: central mitochondria poor (CMP) and superficial mitochondria rich (SMR). The schematic exaggerates the size of the muscle fibres and the proportion of SMR to CMP fibres. In an adult *D. pealeii*, the outer and inner layers of SMR fibres together compose only 4–6% of the thickness of the mantle wall. (C) A schematic of a muscle preparation illustrating the foil clips and the muscle. The gray ovals represent the cut ends of the radial muscle fibres.

Although both fibre types contain a core of mitochondria, SMR muscle fibres have a much larger core with more numerous mitochondria and mainly use oxidative metabolism, while CMP fibres are primarily glycolytic (Bone et al., 1981; Mommsen et al., 1981); (2) an extensive network of capillaries supplies the SMR fibres while the CMP fibres have less vascularisation (Bone et al., 1981); (3) electromyographic recordings in loliginid squids indicate that SMR fibres are active during the low amplitude contractions of the mantle commonly used for respiration and slow jetting while the CMP fibres are quiescent (Bartol, 2001a). In contrast, the CMP fibres are active during rapid jetting (Gosline et al., 1983; Bartol, 2001a).

The distinction between SMR and CMP fibres may not be entirely straightforward. Mommsen and colleagues suggested that enzymatic differences between SMR and CMP fibres vary with lifestyle (Mommsen et al., 1981). For example, unlike the nektonic and pelagic squids in their study, the one benthic species they examined showed few differences in oxidative and glycolytic enzyme activity between the two fibre types. There may be at least two types of CMP fibres that differ in sodium conductance (Gilly et al., 1996).

There are striking differences in the dimensions of the thick myofilaments in the SMR and CMP fibres of the loliginid squid *Sepioteuthis lessoniana*. In newly hatched *S. lessoniana*, the thick filament lengths of both the SMR and CMP fibres average only 1 μm, ranging in length from 0.7 to 1.4 μm (Thompson and Kier, 2006). In juvenile *S. lessoniana*, the thick filament length of the SMR fibres averages 2 μm and ranges up to 4 μm, while the CMP fibres average 1.5 μm but range only up to 2.2 μm (Thompson and Kier, 2006). Thus, there is an ontogenetic increase in thick filament length in *S. lessoniana*, and this increase in the SMR fibres occurs more rapidly than in the CMP fibres. Because thick filament length is proportional to the peak isometric tension generated by a striated muscle fibre but inversely proportional to maximum unloaded shortening velocity (e.g. Josephson, 1975; Kier and Curtin, 2002), differences in thick filament length between SMR and CMP circular muscle fibres may result in differences in contractile properties, assuming other aspects of the two types are similar.

The dimensions of the myofilaments, however, are but one factor that may affect the contractile properties of the SMR and CMP muscle fibres. The contractile properties of striated muscle fibres may be altered in a variety of ways including, but not limited to, expression of different isoforms of the myofilament lattice proteins (e.g. Kendrick-Jones et al., 1976; Sweeney et al., 1988; Marden et al., 1998; Schiaffino and Reggiani, 1996; Toniolo et al., 2007). In contrast to mammals, in which nine myosin heavy chain (MyHC) genes are expressed in skeletal and cardiac muscle and 38 orthologs of MyHC have been putatively identified (Maccatrozzo et al., 2007), only a single MyHC gene has been identified to date in loliginid squid, although it may have two splice variants (Matulef et al., 1998). It is possible, then, that muscle fibre specialization in loliginid squids occurs through alteration in thick filament length, rather than biochemically (Kier and Schachat, 1992; Kier and Curtin, 2002; Kier and Schachat, 2008).

Specific questions addressed

The goals of the present study were to characterize the mechanical properties of the two types of mantle muscle fibres, examine the extent to which thick filament length predicts muscle fibre mechanical properties, and evaluate the roles of the two fibre types in locomotion. We used transmission electron microscopy (TEM) to measure the dimensions of the thick filaments of the SMR and CMP muscle fibres and made predictions about the contractile properties of each fibre type based solely on differences in thick filament length. We tested these hypotheses by measuring contractile properties of partially isolated bundles of SMR and CMP muscle fibres. Finally, we used mantle kinematics data to analyze the roles of the two fibre types in jet locomotion.

MATERIALS AND METHODS

Animals

We studied the superficial mitochondria-rich (SMR) and central mitochondria-poor (CMP) circular muscle fibres of adult long-finned squid *Doryteuthis* (formerly *Loligo*) *pealeii* Lesueur. We chose these animals because the relatively thick (0.1–0.15 mm) SMR and CMP (3–5 mm) fibre layers of *D. pealeii* facilitate experimental manipulation.

We caught male and female *D. pealeii* at night from lighted piers in South Bristol and Walpole, Maine, USA, between 1 June and 10 August 2006. The animals were sexually mature and ranged in size from 112 to 295 mm dorsal mantle length (mean ± s.d.=167±46 mm). Most animals were trapped with a 4.2 m diameter cast net, though some were caught with squid jigs. Squid were housed in a 1 m×2 m×0.5 m tank provided with flow-through seawater at 15°C. The animals were fed small live fish (*Clupea* sp.

and *Notemigonus* sp.) daily. No squid was kept in captivity for more than one week. We used only squid that had no visible damage to the skin or mantle and that appeared to be healthy.

Tissue preparation for mechanical tests

Each squid was killed by decapitation and its mantle transferred immediately to the top of a frozen foam freezer pack. We excised a small portion of the ventral mantle at a position of 1/4 to 1/2 of the dorsal mantle length from the anterior mantle margin. We then peeled the skin from the sample and glued it (using n-butyl cyanoacrylate; Vetbond, 3M, St Paul, MN, USA) to the temperature-controlled stage of a vibratome (Vibratome, St Louis, MO, USA). Immediately after gluing, we filled the bath surrounding the stage with a modified squid saline solution at 4°C. The temperature of the bath was maintained at 4°C for the duration of cutting. The modified solution contained (in mmol l^{-1}): NaCl (450), $MgCl_2 \cdot 6H_2O$ (10), Hepes (10), EGTA (10), pH adjusted to 7.8 with 2 mol l^{-1} NaOH (Milligan et al., 1997).

For the superficial mitochondria-rich (SMR) preparations, we cut sheets of the mantle 0.8–0.1 mm thick using the vibratome. The sheets were cut parallel to the frontal plane of the mantle. Each sheet, therefore, was composed primarily of intact circular muscle fibres, though fragments of radial muscle fibres and connective tissue fibres were also present (Fig. 1). We made no attempt to remove the outer tunic.

Using the vibratome allowed us to isolate SMR and CMP fibres in different muscle preparations and also severed the radial muscles fibres, thereby interfering with their ability to contract. It is important to note, however, that mantle is a complex, muscular organ. Although we took care to segregate SMR and CMP fibres into two types of preparations, we conducted tests on tissue preparations that included both muscle and short sections of connective tissue fibres. Nonetheless, we believe the preparations were suitable for highlighting important mechanical differences between the two muscle fibre types.

We trimmed the mantle sheets into pieces 5–10 mm long and 2–4 mm wide. We glued T-shaped foil clips (Milligan et al., 1997) to each end of the mantle slice using Vetbond (Fig. 1C) and then transferred the preparation to a temperature-controlled muscle bath. The muscle bath was filled with standard squid saline containing (in mmol l^{-1}): NaCl (470), KCl (10), $CaCl_2$ (10), $MgCl_2 \cdot 6H_2O$ (50), Glucose (20), Hepes (10), pH adjusted to 7.8 with 2 mol l^{-1} NaOH (Milligan et al., 1997). The temperature of the muscle bath was maintained at 20±0.2°C. This temperature was 5–7°C warmer than the seawater from which the *D. pealeii* squid were captured but was within the normal range of temperatures encountered by this species in the field. We chose 20°C, partly because preparation survival was higher than at 13–15°C and partly because we hope in the future to compare the results of experiments on the CMP fibres between *D. pealeii* and two other species of loliginid squids that live in 20–27°C water.

For CMP preparations, we cut 0.1–0.15 mm thick sheets from the central zone of the mantle (Fig. 1) with the vibratome, trimmed them, and then attached foil clips as described above. We were unable to compare SMR and CMP preparations from the same animal.

Muscle mechanics experiments

Once in the muscle bath, one foil clip was attached to a force transducer (404A Transducer System, Aurora Scientific, Ontario, CA, USA) and the other to a computer-controlled servomotor (322C Muscle Lever System, Aurora Scientific). We allowed muscle preparations to equilibrate in the standard squid saline for 30 min prior the start of the experiment.

We followed the protocols outlined elsewhere (Milligan et al., 1997; Kier and Curtin, 2002) for conducting the mechanical tests. We stimulated the muscle preparations with rectangular constant current pulses *via* platinum plate electrodes that were of sufficient size to cover the length of preparation. The length–force relationship of the preparation was determined using supramaximal brief tetanic (2 ms pulses, 50 Hz, 200 ms duration) and twitch stimulations. Once we determined the length (L_0) of the preparation that yielded peak tetanic force (P_0), we next studied the stimulus frequency–force relationship using brief tetani (2 ms pulse, 200 ms duration, 300 s between successive tetani) at a range of frequencies between 1 and 500 Hz. We calculated the peak tetanic stress of the fibres by dividing P_0 by the physiological cross section of the preparation (see following sections for details). With the preparation maintained at L_0, we then used slack step tests (Edman, 1979) to estimate the maximum unloaded shortening velocity (V_{max}) in brief tetanus. We used four different step lengths for each preparation that varied from 1% to 6% of L_0. Step length data were plotted against the corresponding time of force recovery. The data were fit with a linear regression. The slope of the regression was the maximum unloaded shortening velocity (Edman, 1979). Each slope was then divided by L_0 to normalize for variations in preparation length. We conducted all of the above tests on seven SMR and ten CMP preparations.

We also analyzed three temporal aspects of the brief tetanic contraction at L_0. First, we measured the latent period (T_L) as the time from the beginning of the first rectangular pulse stimulation to the initial rise in force (see Fig. 5B for illustrations). Second, we measured the time to peak (T_P) as the initial rise in force to the peak force produced. Finally, we measured the time required for force to fall from the peak to 50% peak (T_{50}).

We performed regular isometric control stimulations to monitor the health of the preparation. If the force produced during isometric contraction at L_0 decreased by more than 10%, we terminated the experiment and discarded all data collected subsequent to the previous control stimulation.

Control for radial muscle function

The radial muscles serve as antagonists to the circular muscles. The muscle preparations we studied were composed of both circular fibres and fragments of radial fibres. Simultaneous contraction of both fibre types may have affected the magnitude of force produced by the circular muscles. Therefore, we treated several of our preparations with 20 μmol l^{-1} acetylcholine mixed in standard squid saline. Because acetylcholine serves as a neurotransmitter for radial muscles but not for the circular muscles, any change in the dimensions of the muscle preparations would have indicated radial muscle shortening (Bone et al., 1982; Collins and Tsutsui, 2003). We saw no measurable change in any of the preparations and therefore concluded that vibratome sectioning disabled the radial muscle fibres.

Determination of physiological cross section of the fibre preparations

Immediately following the mechanical testing, the preparations were fixed at L_0 at 4°C in either 3.0% glutaraldehyde, 0.065 mol l^{-1} phosphate buffer, 0.5% tannic acid and 6% sucrose (Kier, 1985) or modified Karnovsky's fixative [2.5% paraformaldehyde, 3% glutaraldehyde, 0.065 mol l^{-1} phosphate buffer and 2.5% sucrose (Bozzola and Russell, 1992)] for 12–24 h. The tissue was rinsed in chilled 0.065 mol l^{-1} phosphate buffer for 30 min, dehydrated in a

graded series of ethanol up to 95%, and then embedded in glycol methacrylate plastic (JB-4 Plus, Polysciences, Inc., Warrington, PA, USA). The tissue blocks were sectioned at 0.5–1.0 μm in a plane perpendicular to the long axes of the circular muscle fibres and stained in an aqueous solution of 0.1% Toluidine Blue and 0.1% sodium borate.

The stained slides were photographed under bright-field microscopy. Both the total cross sectional area of the preparation and the portion occupied by radial muscles were measured using ImageJ (public domain software; National Institutes of Health, USA). We then subtracted the radial muscle area from the total cross-sectional area to get the physiological cross section. The physiological cross section, therefore, included the areas occupied by the myofilaments and the core of mitochondria of the circular muscle fibres.

Determination of thick filament lengths

A small piece of the fixed tissue preparation was post-fixed for 45 min at 4°C in a 1:1 solution of 2% osmium tetroxide and 2% potassium ferrocyanide in 0.13 mol l^{-1} cacodylate buffer (Kier, 1985). The tissue was rinsed in chilled 0.13 mol l^{-1} cacodylate buffer for 15 min, dehydrated in a graded series of acetones and embedded in epoxy resin.

The processes of fixation, dehydration and embedding may cause shrinkage of cells and connective tissues. A-band lengths of various frog cross-striated skeletal muscles suffered minimal shrinkage relative to other methods when fixed in buffered glutaraldehyde and dehydrated in acetone (Page and Huxley, 1963). Thus, we adopted their protocol to minimize the effects of tissue processing on myofilament lengths.

We followed the protocol (Thompson and Kier, 2006) for measuring thick filament lengths. Briefly, embedded tissue blocks were sectioned in a plane perpendicular to the longitudinal axis of the mantle (i.e. parallel to the long axes of the circular muscles) using a diamond knife. Thick sections (0.5–1 μm) were cut initially and stained in an aqueous solution of 0.1% Methylene Blue and 0.1% Azure II. Sections were then examined using bright-field microscopy to determine if the long axes of the circular muscle fibres were parallel to the knife edge. Once alignment was achieved, thin sections (silver interference color) were cut, mounted on grids, and stained with 2% aqueous uranyl acetate (Bozzola and Russell, 1992) and 0.4% lead citrate (Venable and Coggeshall, 1965). Thin sections were examined with a Zeiss EM-902 transmission electron microscope and portions of the sections that met our criteria (see below) were photographed.

Because the circular muscle fibres of squid are fusiform in shape (Bone et al., 1995) and obliquely striated (Hanson and Lowy, 1957; Lowy and Hanson, 1962; Millman, 1967), it is often difficult to confirm that the section plane is parallel to the longitudinal axis of the fibre and thus to ensure that an individual thick filament remains in the section plane along its entire length. As described above, an attempt was made to carefully align the section plane during ultramicrotomy, and care was taken to measure thick filaments only from fibres (1) in which the diameter of the mitochondrial core remained constant over the length of the fibre (suggesting that the long axis of the fibre was parallel to the section plane) and (2) that spanned at least two bars of a 300 mesh grid. Because of the difficulties associated with section plane alignment, however, the thick filament lengths we report here may be underestimates.

The electron micrograph negatives were scanned at 4800 d.p.i. and thick filament lengths measured using ImageJ software. We measured thick filaments from at least five muscle fibres per preparation. We measured a total of 270 thick filaments from SMR fibres and 260 from CMP fibres from 5 animals. The mean thick filament length per fibre type per animal was used for the statistical comparisons.

Determination of cross-sectional areas of individual muscle fibres

To analyze the cellular basis for differences in the mechanical properties of the SMR and CMP muscle fibres, we measured cross-sectional areas of (1) the whole fibre, (2) the area occupied by the myofilaments and (3) the mitochondrial core from transmission electron micrographs of cross sections of the muscle cells. Because both the SMR and CMP fibres taper longitudinally and adjacent fibres are not in register, cross sections of the cells reveal fibres of different sizes and with different relative mitochondrial and myofilament areas. In an attempt to correct for this variability, we measured the cross-sectional areas of each cell, its myofilaments, and its mitochondrial core for every circular fibre visible in the photomicrograph. We presented the data using box plots to provide a better overview of the variability in the muscle fibres. We measured approximately 40 SMR and 40 CMP fibres from each of 5 animals.

We also used ImageJ software to estimate the aggregate cross sectional area of the sarcoplasmic reticulum (SR) in each of the muscle cells we measured above. It is important to emphasize that the SR data we report are not estimates of the volume fraction of SR, but are indicative of the relative proportion of SR in each muscle fibre type.

Statistics

The SMR and CMP morphometric and mechanical data were distributed normally. We used a one-way ANOVA with Tukey's honestly significant difference (HSD) *post hoc* test for all comparisons.

RESULTS

Morphometrics of mantle muscle fibres

Superficial mitochondria-rich (SMR) circular muscle fibres had significantly longer thick filaments than the central mitochondria-poor (CMP) fibres (P<0.001; Figs 2, 3). The mean ± s.d. lengths of SMR and CMP thick filaments were 3.12±0.56 μm and 1.78±0.27 μm, respectively.

The cross-sectional areas occupied by the myofilaments, the mitochondrial core, and the whole muscle fibre for SMR and CMP fibres are indicated in Fig. 4. The median cross sectional areas of whole fibres (P<0.001) and the mitochondrial core (P<0.001) differed significantly between SMR and CMP muscle fibres (Fig. 4). It is noteworthy that the cross sectional area of the myofilaments was not significantly different (P=1; Fig. 4).

The amount of sarcoplasmic reticulum visible in cross sections was significantly higher in CMP fibres (mean ± s.d.=5.5±2.6%) than in SMR fibres (0.97±0.22%, P=0.009).

The radial muscle fibres occupied a mean of 18.2±2.7% (N=17) of the total cross-sectional area of the muscle preparations. Regression analysis indicated no relationship between the proportion of radial muscles and dorsal mantle length (P=0.94, data not shown) for our sample population.

Mechanical properties of muscle fibres

Using regression analysis (data not shown) we were unable to detect relationships between dorsal mantle length (DML) of the squid and any of the following variables: maximum unloaded shortening velocity (V_{max}), peak isometric stress (P_0), twitch:tetanus (Tw:Tt)

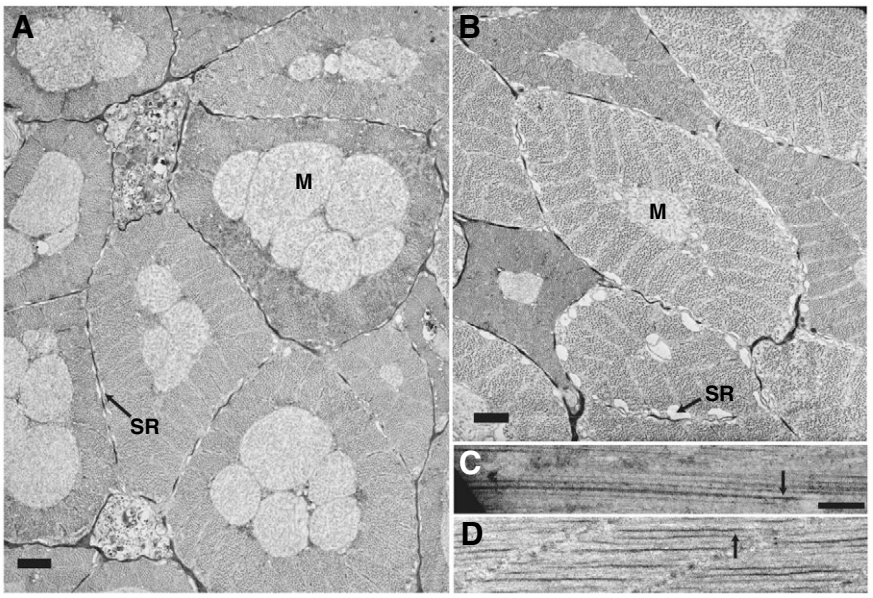

Fig. 2. Electron micrographs of cross sections of SMR (A) and CMP (B) circular muscle fibres to illustrate differences in the cells. Note the large core of mitochondria (M) in the SMR fibres and the more extensive sarcoplasmic reticulum (arrows) in the CMP fibres. Scale bars, 2 μm (A); 1 μm (B). (C,D) Electron micrographs of longitudinal sections of the SMR (C) and CMP (D) circular muscle fibres. Scale bar for C and D, 0.5 μm. Note the longer thick filaments (arrows) in the SMR fibre.

ratio, the stimulus frequency that elicited maximum force, or the time course of the contraction. Therefore, we did not segregate data by body size.

The mean P_0 of the SMR preparations was significantly higher than that of the CMP preparations (P<0.001; Fig. 5, Fig. 6A). P_0 range was 190–250 mN mm^{-2} physiological cross section (pcs) and 272–378 mN mm^{-2} pcs for CMP and SMR preparations, respectively. The stimulation frequency that elicited P_0 was significantly higher in SMR (441±37 Hz) preparations than in CMP (400±15 Hz) preparations (P=0.026), but the relevance of this difference is uncertain given that both SMR and CMP preparations were stimulated within 10% of P_0 at a stimulation frequency of about 150 Hz. The Tw:Tt ratio was significantly lower in SMR preparations than in CMP preparations (P=0.046; Fig. 5, Fig. 6B).

All the slack tests resulted in close relationships between step length and force recovery time (see Fig. 7A for two examples). The mean V_{max} of SMR fibre preparations was significantly lower than CMP preparations (P=0.0006; Fig. 7B). V_{max} range was 3.5–6.8 L_0 s^{-1} and 1.6–3.7 L_0 s^{-1} for the CMP and SMR preparations, respectively.

There were no significant differences in the time course of force generation during brief tetanic stimulation between SMR and CMP muscle preparations (Table 1).

The passive tension at L_0 was substantially higher in all of the SMR preparations than in the CMP preparations (Fig. 8).

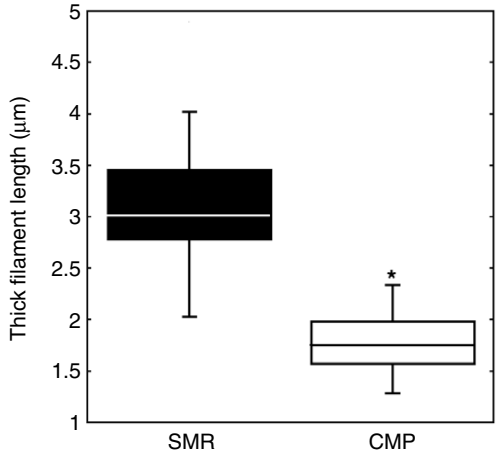

Fig. 3. Thick filament length in the two types of muscle fibres. The thick filaments of the SMR fibres (black) were significantly longer than those of the CMP fibres (white) (ANOVA with Tukey HSD *post hoc* test). The box plots illustrate the median (the horizontal line), the upper and lower quartile (the box), and the range of the data (the 'whiskers'). There were no outliers. We measured 270 SMR thick filaments and 260 CMP thick filaments from 5 animals. *Significantly different (P<0.001).

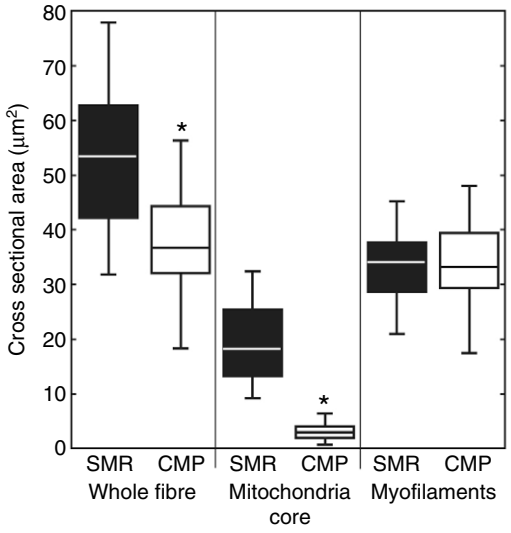

Fig. 4. Comparison of cross sectional areas of the whole fibre, the core of mitochondria, and the myofilaments between SMR (black) and CMP (white) fibre preparations. The plots illustrate the median (the horizontal line), the upper and lower quartile (the box), and the range of the data (the 'whiskers'). There were no outliers. Approximately 40 SMR and 40 CMP fibres were measured from each of five different animals. *Significantly different (P<0.001; ANOVA with Tukey HSD *post hoc* test).

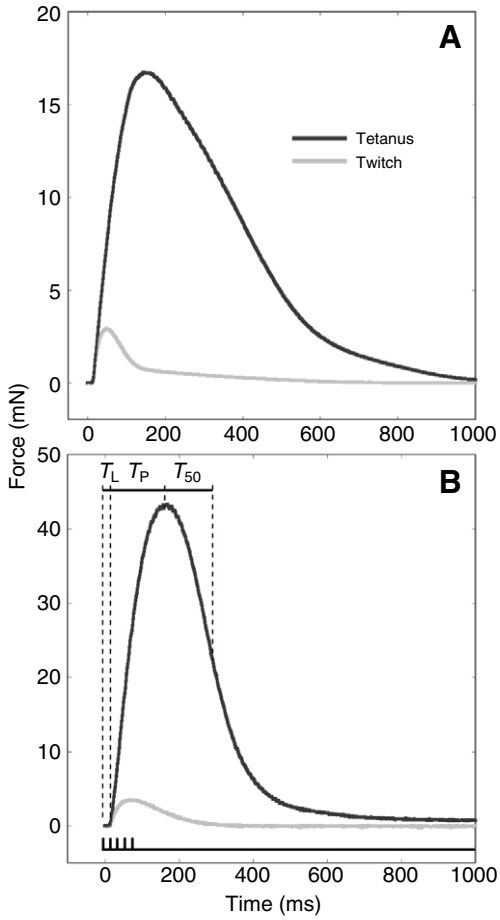

Fig. 5. Force–time relationship in twitch (2 ms pulse, 1 Hz; gray line) and tetanus (2 ms pulse, 400 Hz, 100 ms duration; black line) for CMP (A) and SMR (B) preparations. The tetanus trace in B also illustrates the temporal aspects of force that we measured. The lowest black line illustrates the timing of electrical stimuli. Please note that the scale of the time axis does not permit accurate depiction of the timing of electrical stimuli. T_L, latent period, measured as the time from the beginning of the first rectangular pulse stimulation to the initial rise in force; T_P, time from the initial rise in force to the peak force; T_{50}, time required for force to fall from the peak to 50% peak.

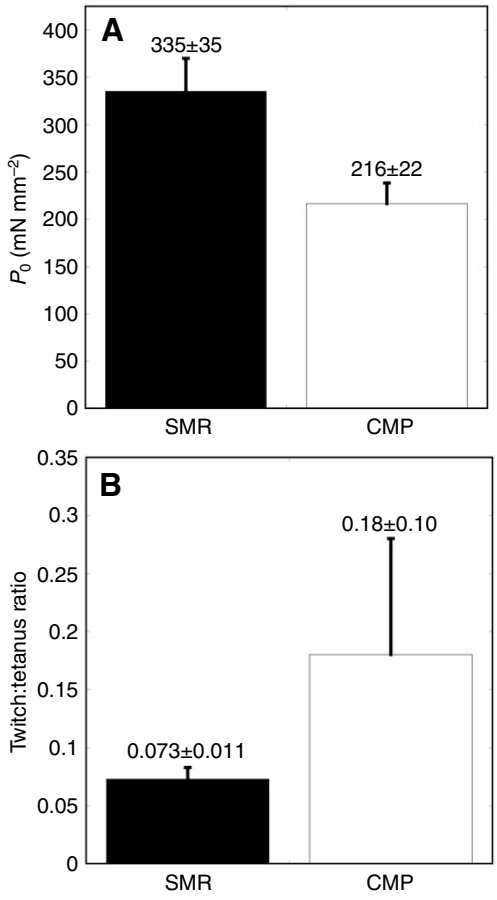

Fig. 6. Variation of peak isometric stress (A) and twitch:tetanus ratio (B) between the two different muscle fibre preparations in tetanus (400 Hz, 100 ms) at 20°C. CMP fibres produced significantly less isometric stress than SMR fibres (P<0.0001; ANOVA with Tukey HSD *post hoc* test). CMP fibres had a significantly higher twitch:tetanus ratio than SMR fibres (P=0.046; ANOVA with Tukey HSD *post hoc* test). The numbers above each bar are the mean ± s.d. P_0 is reported as mN mm^{-2} physiological cross section.

DISCUSSION

Comparison of the peak isometric stress of the central mitochondria-poor (CMP) and superficial mitochondria-rich (SMR) fibres is complicated by the large difference in the size of the core of mitochondria in these muscles. About 64% and 92% of the total cross-sectional area of the cell is occupied by myofilaments in SMR and CMP fibres, respectively. If we subtract the cross-sectional areas of the mitochondrial cores of the SMR and CMP fibres from the physiological cross section, the SMR and CMP fibres produce peak isometric stresses of 523 and 234 mN mm^{-2} physiological cross section, respectively. The corrected P_0 for the CMP fibres is comparable to the white muscle fibres of dogfish (Curtin and Woledge, 1988) and the fast twitch fibres of frogs (Curtin and Edman, 1994). Both the uncorrected (Fig. 6A) and corrected P_0 for the SMR fibres are much higher than values reported for their hypothetical analogues (Mommsen et al., 1981): the aerobic red muscles of fishes (e.g. Swank et al., 1997; Young and Rome, 2001). This is not surprising given that the thick filaments of the SMR fibres of *D. pealeii* are more than two times longer than the thick filaments of the red muscles of fishes [e.g. carp (Sosnicki et al., 1991)].

The twitch:tetanus (Tw:Tt) ratio for the CMP fibres of *D. pealeii* was identical to that of the CMP fibres of *A. subulata* (Milligan et al., 1997) but the Tw:Tt ratio of the SMR fibres was significantly

Table 1. Temporal aspects of the contraction of CMP and SMR fibres

	SMR	CMP	P
T_L (ms)	4.6±1.4	4.4±1.5	0.78
T_P (ms)	143±28.9	143±57.7	0.98
T_{50} (ms)	135±28.4	175±98.9	0.22
N	7	10	

Comparison of the temporal aspect of the contraction of SMR and CMP preparations in brief tetanus (2 ms pulse, 50 Hz, 100 ms duration). T_L, latent period between the first stimulation and rise in force; T_P, time from the rise in force to the peak force; T_{50}, time from peak force to 50% peak force.

Values are mean ± s.d. There were no significant differences between SMR and CMP preparations (P>0.05; Tukey HSD test).

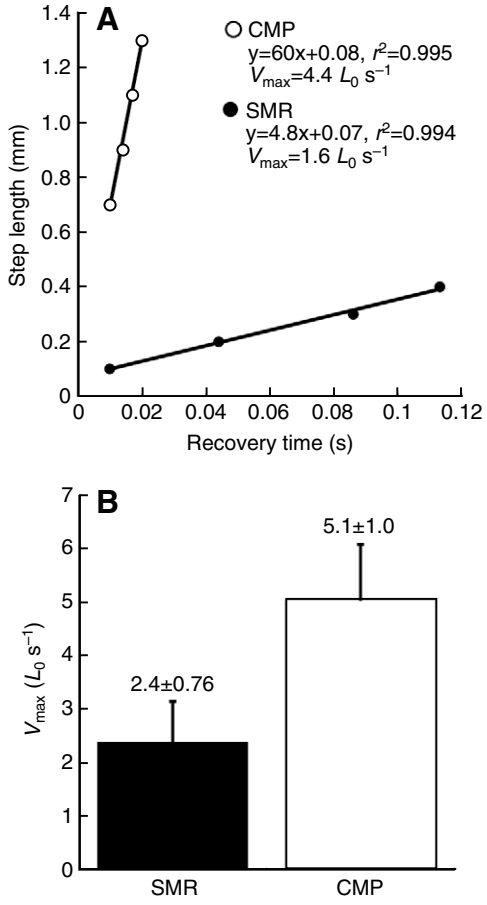

Fig. 7. Comparison of maximum unloaded shortening velocity (V_{max}) in brief tetanus (50 Hz, 100 ms) at 20°C. (A) Slack step test data for one CMP (open circles) and one SMR (filled circles) preparation. (B) Maximum unloaded shortening velocity for the two different muscle fibre preparations. The numbers above each bar are the mean ± s.d. CMP fibres had a significantly higher V_{max} than SMR fibres (P=0.0003; ANOVA with Tukey HSD *post hoc* test).

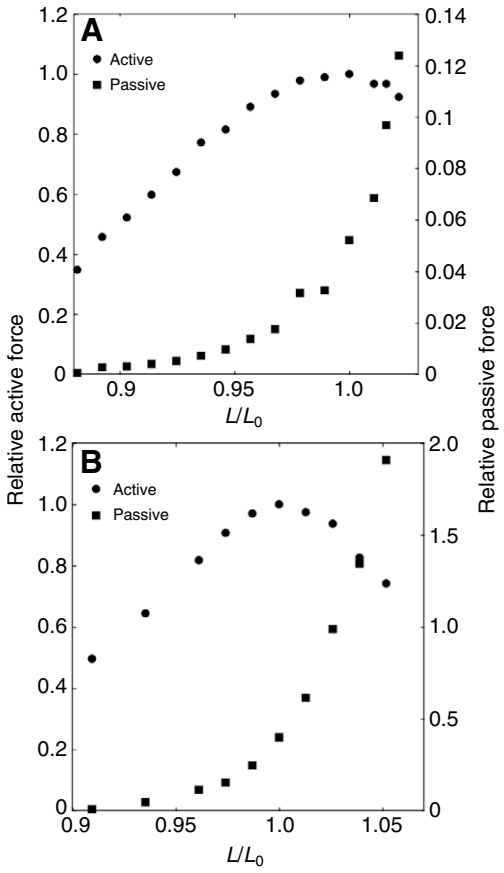

Fig. 8. Comparison of typical active (in brief tetanus) and passive forces for CMP (A) and SMR (B) preparations. Note that the passive force is higher in the SMR than in the CMP preparations.

lower. This implies that the pattern of activation of the two muscle types may be different *in vivo*. Circumstantial evidence suggests that the SMR fibres are innervated by the non-giant motor system (Prosser and Young, 1937; Young, 1938; Brown et al., 1991). The CMP fibres of the market squid *Loligo opalescens* are innervated by both the giant and non-giant systems (Otis and Gilly, 1990), although it remains unclear if each CMP muscle cell receives dual innervation or if populations of CMP fibres are innervated by one system or the other.

There was an approximately twofold difference in shortening velocity between the SMR and CMP fibres. Although shortening velocity varies with the load on the muscles and we have no information on the loads experienced in the mantle, it is likely that the CMP fibres shorten more rapidly than the SMR fibres *in vivo*. The V_{max} we found for the CMP fibres is comparable to that of another loliginid squid, *Alloteuthis subulata* (Milligan et al., 1997), assuming that the Q_{10} of squid muscle is about 2.0.

Despite the significantly greater area of sarcoplasmic reticulum (SR) visible in the cross sections of the CMP muscle fibres we found no differences in the time course of muscle contraction during brief tetanus (Table 1) or in the minimum current required to elicit maximal contraction between the two preparation types. Although the volume fraction of SR present in a muscle cell correlates with fibre type in vertebrates (Eisenberg, 1983) and relaxation rate, a thorough analysis of E–C coupling is required before a complete comparison of SMR and CMP fibres can be made. Fast Na^+ channels have been found putatively in the CMP fibres of *L. opalescens* (Gilly et al., 1996) and in *A. subulata* (Rogers et al., 1997), but it is unknown if they are present in the SMR fibres as well.

It is noteworthy that none of the temporal aspects (T_L, T_P, T_{50}) that we measured differed between the two fibre types. Studies of *D. pealeii*, *L. opalescens* and the brief squid *Lolliguncula brevis* indicate that the period of the jet changes little as swimming speed increases (O'Dor, 1988; Anderson and DeMont, 2000; Bartol, 2001b). As a squid jets faster, the refilling times become shorter, presumably as radial muscle activity increases to speed refilling (Gosline et al., 1983), and the amplitude of mantle contraction may increase (Anderson and DeMont, 2000), but the time course of mantle contraction does not change dramatically. Thus, the similarity in the temporal aspects of isometric contraction that we noted appears consistent with mantle kinematics.

Passive tension and effect of the tunic

We were unable to remove the outer tunic from the SMR preparations and it is possible that this thin (ca. 25 μm) layer of collagen fibres affected passive tension in the preparations, V_{max}, and the temporal aspects of isometric contraction. The passive tension at L_0 was substantially higher in all of the SMR preparations

compared with the CMP preparations (Fig. 8). Examination of the SMR preparations with polarized light microscopy revealed that the long axes of the collagen fibres in the outer tunic were approximately 60° to the long axes of the circular muscle fibres (data not shown). Because there is no discernable difference in the distribution of intramuscular connective tissue fibres across the mantle wall (Thompson and Kier, 2001), we attribute the difference in passive tension to the presence of the tunic. Although the tunic may have contributed to passive tension, there are several reasons why it is unlikely to have affected V_{max} or the temporal aspects of isometric contraction. First, for three of the SMR preparations we conducted slack step tests at preparation lengths that were shorter than L_0. At these shorter lengths, passive tension was zero and the mean V_{max} of the three SMR fibres was little different from the V_{max} at L_0. Second, we had numerous preparations that contained the tunic as well as both SMR and CMP fibres. In these mixed fibre preparations (which were excluded from all of the other analyses), V_{max} varied inversely with the percentage of SMR fibres in the preparation (Pearson's R=–0.6, P=0.01, N=20), despite the presence of the tunic. Therefore, it is unlikely that elastic recoil of the tunic fibres affected V_{max}. Third, there were no significant differences in the temporal aspects of isometric contractions between the mixed SMR/CMP preparations and either the 'pure' SMR or CMP preparations (data not shown).

Do ultrastructural differences explain mechanical differences?

In striated muscles including, presumably, obliquely striated circular muscles, thick filament length is proportional to the peak isometric stress (P_0) of the fibre (e.g. Josephson, 1975; Kier and Curtin, 2002). Thus, the longer thick filaments of the SMR fibres should increase the P_0 produced relative to the CMP fibres. Consistent with this hypothesis, we found that the P_0 of SMR fibres was, indeed, significantly greater than that of the CMP fibres. Because maximum unloaded shortening velocity (V_{max}) is inversely proportional to thick filament length (e.g. Josephson, 1975; Kier and Curtin, 2002), the longer thick filaments of SMR fibres should be correlated with slower V_{max}. Consistent with this hypothesis, we found that V_{max} was significantly slower in the SMR fibres.

But do the differences in thick filament length alone explain the differences in the contractile properties of the SMR and CMP circular muscle fibres of *D. pealeii*? The thick filaments of the SMR fibres are about 1.75 times longer than those of CMP fibres (Figs 2, 3). Thus, if other aspects of the two fibre types are the same, and if the relationship between thick filament length and isometric stress is linear, the P_0 of SMR fibres should be 1.75 times greater than the P_0 of CMP fibres. The P_0 of the SMR fibres was approximately 1.5 times greater (Fig. 6A), but if we correct for differences in the size of the core of mitochondria, the P_0 is about two times greater. By similar reasoning, the V_{max} of the SMR fibres should be 1.75 times slower than the CMP fibres, and it is approximately two times slower (Fig. 7B).

We cannot exclude the possibility that different isoforms of the myofilament lattice proteins are expressed in SMR and CMP fibres. The obliquely striated muscles of squid have received scant attention relative to other striated muscles and little is known about the isoforms of contractile proteins present in the mantle. Matulef and colleagues (Matulef et al., 1998) found evidence for two isoforms ('A' and 'B') of myosin heavy chain in the funnel retractor muscle of *D. pealeii* that may be splice variants of a single gene. The putative splice variants differ in the amino acid sequence of the ATP binding region (Matulef et al., 1998); thus, the splice variants may affect V_{max}. There is no evidence that both variants are expressed in the mantle, though RT-PCR analysis of the arms and tentacles of *D. pealeii* indicated that one isoform ('A') composes more than 95% and 90% of the total myosin heavy chain in the arms and tentacles, respectively (Kier and Schachat, 2008). Limited information about a few other myofilament lattice proteins involved in shortening is available. Konno (Konno, 1978) purified myosin, tropomyosin and three troponins from the mantle of an ommastrephid squid (*Todarodes pacificus*). Unfortunately, the methods used by Konno were inappropriate to determine if isoforms of any of the isolated proteins were present. Ojima et al. determined the amino acid sequence of troponin C in *T. pacificus*, but did not find isoforms (Ojima et al., 2001). Additional work is still needed to determine the full extent of specialization between CMP and SMR fibres. We are currently studying potential myosin heavy chain isoforms in the mantle. Nevertheless, our results are consistent with the prediction that structural differences play a primary role in determining the differences in the mechanical properties of the two types of circular muscle fibres.

Functional significance of circular muscle specialization

The differences in mechanical properties of the two types of circular muscle fibres may have a number of significant effects on mantle kinematics and jet locomotion.

Muscle 'gears'

The SMR and CMP fibres follow parallel trajectories through the mantle. In this way, there does not appear to be an 'architectural gear ratio' (*sensu* Brainerd and Azizi, 2005) between the SMR and CMP fibres as there is between the red and white muscle fibres of fishes (Alexander, 1968; Rome and Sosnicki, 1991; Wakeling and Johnston, 1999) and the various layers of hypaxial muscle in *Siren lacertina* (Brainerd and Azizi, 2005). Nevertheless, the twofold difference in P_0 and V_{max} between the SMR and CMP fibres suggests that the mantle does have at least two muscle 'gears'. Simultaneous mantle kinematics and electromyographic (EMG) recordings in the brief squid *Lolliguncula brevis* are consistent with the idea that the two fibre types are differentially recruited as swimming speed increases. Bartol (Bartol, 2001a) observed no CMP electrical activity at <1 DML s^{-1}, both SMR activity and sporadic CMP activity at 1–3 DML s^{-1}, and continual CMP activity at >3 DML s^{-1}. Thus, the aerobic SMR and anaerobic CMP (Bone et al., 1981; Mommsen et al., 1981) fibres may represent low and high 'gears', respectively.

Strain and strain rate predictions from a simple mantle model

Consideration of the geometry of the mantle shows that circular muscle fibre strain and strain rate vary as a function of location in the mantle wall; strain and strain rate increase from the outer (i.e. the side covered by the skin) to the inner (i.e. the side in contact with the mantle cavity) surface. This transmural gradient arises because (1) the mantle is circular in cross section, (2) the mantle wall is constant in volume (Ward, 1972), and (3) the length of the mantle either does not increase when the circular muscles contract (Ward, 1972) or increases by less than 5% (Packard and Trueman, 1974). As the circular muscle fibres contract, therefore, the mantle not only decreases in diameter but the mantle wall thickness increases (Fig. 9). Transmural variation in strain and strain rate has several interesting implications for mantle muscle function. Do SMR and CMP fibres near the outer surface of the mantle operate on a different portion of the length–tension curve than those near the inner edge? Within the CMP fibres, does power output vary across

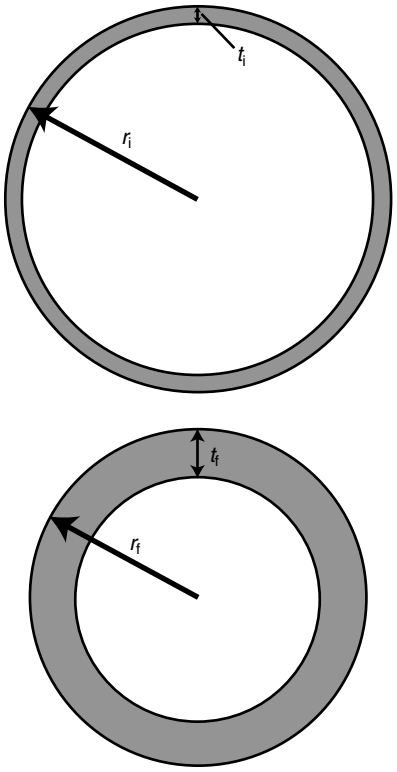

Fig. 9. Illustration of how mantle diameter and thickness change during a jet. The lower schematic slightly exaggerates the increase in mantle wall thickness that occurs as the mantle contracts. t_i, initial (i.e. resting) mantle wall thickness; t_f, final wall thickness (i.e. at the end of contraction during the exhalant phase of the jet); r_i, initial radius of the outer edge of the mantle; r_f, the final radius of the outer edge of the mantle.

the mantle wall? Although our data do not permit direct answers to these questions, modeling of the dimensional changes of the mantle during jetting allows prediction of mantle muscle strain rate and strain and thus provides insight.

To explore the relationship between the transmural gradient of strain and strain rate and the contractile properties of the CMP and SMR circular muscle fibres, we constructed a simple model based on a transverse slice of the mantle. The dimensions of the model slice were based on measurements of mantle diameter and mantle wall thickness at ½DML from an adult *D. pealeii* (DML, 150 mm) anesthetised in a 1:1 solution of 7.5% $MgCl_2$:seawater (Messenger et al., 1983). The anesthetic relaxed the circular muscles, resulting in mantle dimensions similar to those observed just prior to the start of the exhalant phase (i.e. the portion of the jet in which water is forced out of the funnel by contraction of the circular muscles) of the jet (see Thompson and Kier, 2001).

We selected three jetting speeds for comparison: slow (~0.5 DML s^{-1}), intermediate (~2 DML s^{-1}), and fast (an escape jet at 12 DML s^{-1}). We do not have coordinated mantle kinematics and EMG data for *D. pealeii*, but in *L. brevis* the SMR fibres alone are active at slow swimming speeds <1 DML s^{-1}, while the CMP fibres are active sporadically at intermediate speeds (1–3 DML s^{-1}) and constantly at high speeds [>3 DML s^{-1} (Bartol, 2001a)]. We presume that the speeds we selected, then, represent situations in which power for the jet is provided by the SMR fibres alone (slow), both the SMR and CMP fibres (intermediate), and the CMP fibres alone (fast). We measured the amplitude of mantle contraction and the period of the exhalant phase of the jet during slow, intermediate and escape jets from the high-speed (250 frames s^{-1}) video sequences of another specimen of *D. pealeii* (DML, 152 mm). During the exhalant phase of the jet, the diameter of the mantle decreased 5% over 0.3 s, 12% over 0.25 s and 25% over 0.15 s, for the slow, intermediate and escape jets, respectively (J. T. Thompson, P. S. Krueger and I. K. Bartol, in preparation). Hyperinflation (Gosline et al., 1983) of the mantle was not apparent in the jets we evaluated.

We combined the morphological and kinematics data to calculate the mantle wall thickness at the end of a jet (see Appendix and Fig. 9). We then calculated circumferential strain and strain rate ($\dot{\varepsilon}$, in mantle circumference lengths s^{-1}) at the outer and the inner edges of the mantle wall. The results of the calculations are listed in Table 2 and the initial conditions and values used for the calculations are provided in Table 3. The model predicts that the circular muscle fibres near the inner surface of the mantle wall experience 1.3- and 1.4-fold higher strain and strain rates during slow jetting and escape jetting, respectively, than fibres near the outer surface. The model also shows that the greater the thickness of the mantle wall relative to the radius of the mantle, the greater the difference in transmural strain and strain rate for the inner *versus* the outer surface (see Appendix).

The model also predicts that both the SMR and CMP circular muscle fibres experience high strains at intermediate and higher

Table 2. Transmural strain and strain rate prediction

	Slow jet	Intermediate jet	Escape jet
ε_{out}	0.05	0.15	0.25
ε_{in}	0.068	0.21	0.36
$\dot{\varepsilon}_{out}$ (L s^{-1})	0.14	0.60	1.70
$\dot{\varepsilon}_{in}$ (L s^{-1})	0.19	0.84	2.41
SMR $\dot{\varepsilon}/V_{max}$	0.06–0.08	0.25–0.35	0.71–1.0
CMP $\dot{\varepsilon}/V_{max}$	0.03–0.037	0.12–0.16	0.33–0.47

Illustration of transmural differences in strain and strain rate predicted by a simple model (see Appendix). The values are based on measurements of mantle diameter and thickness from an anesthetised adult *D. pealeii* (dorsal mantle length, DML, 150 mm), and mantle kinematics recorded from a different, but similar sized, animal. Speed of swimming and the percentage decrease in the outer diameter of the mantle for the different jets: slow jet (~0.5 DML s^{-1}; 5%); intermediate jet (~2 DML s^{-1}; 15%); escape jet (12 DML s^{-1}; 25%). ε_{out}, circumferential strain at the outer edge of the mantle; ε_{in}, circumferential strain at the inner edge of the mantle; $\dot{\varepsilon}_{out}$, strain rate at the outer edge of the mantle in mantle circumference lengths s^{-1} (L s^{-1}); $\dot{\varepsilon}_{in}$, strain rate at the inner edge of the mantle. Mean V_{max} for the SMR and CMP fibres taken from Fig. 7B.

Table 3. Values used for the simple mantle model

	At rest	Slow jet	Intermediate jet	Escape jet
r_i (mm)	25.0	25.0	25.0	25.0
r_f (mm)	–	23.75	21.25	18.75
t_i (mm)	3.5	3.5	3.5	3.5
t_f (mm)	–	3.71	4.25	5.0
Δt (s)	–	0.35	0.25	0.15

Initial conditions for the model, based on measurements of an anesthetised *D. pealeii* and mantle kinematics data for three jetting speeds (see Table 2). The calculations are described in the Appendix. r_i, initial radius of the outer edge of the mantle (i.e. the mantle at rest); r_f, final radius of the outer edge of the mantle (i.e. at the end of the exhalant phase of the jet); t_i, initial thickness of the mantle wall; t_f, final thickness of the mantle wall; Δt, period of the exhalant phase of the jet.

jetting speeds (Table 2). The cross-striated muscle fibres of the vertebrates appear to experience relatively low strains, especially during locomotion (Burkholder and Lieber, 2001). For example, the red muscles of carp experience maximum strain of 0.14 during sustainable swimming speeds, and the strain of white muscles during escape responses is 0.18 (van Leeuwen et al., 1990; Rome and Sosnicki, 1991). Moreover, these strains are nearly centered on the fibre length (L_0) that produces the highest force (Rome and Sosnicki, 1991). One problem with our model, and with studies of obliquely striated muscles in general, is that we cannot yet relate mantle circumference to L_0 and, thus, cannot determine where on the length–tension curve the different muscle fibres operate. This issue is currently under investigation.

Milligan et al. (Milligan et al., 1997) calculated power output from the force–velocity relationship of the CMP fibres of the loliginid squid *Alloteuthis subulata*. They noted that peak power output occurred at V/V_{max} of about 0.38 and that the fibres produced high power over a fairly broad range of lengths, particularly compared to the cross striated fibres of a variety of vertebrates (Lännergren et al., 1982; Curtin and Woledge, 1988; Rome and Sosnicki, 1990; McLister et al., 1995). We estimated V/V_{max} by using the strain rates ($\dot{\varepsilon}$) calculated from the model as a proxy for the *in vivo* shortening velocity (V) of the circular fibres and the mean V_{max} data from Fig. 7B. If peak *in vitro* power at a V/V_{max} of 0.38 occurs also in the SMR and CMP fibres of *D. pealeii*, the model predicts that SMR fibre power output peaks near the likely recruitment speed of the CMP fibres (Table 2). The model also predicts that the CMP fibres generate virtually no power for slow jetting while the SMR fibres are too slow to generate power for escape jets. The transmural variation in strain and strain rate suggests that different regions of the mantle produce different amounts of work during locomotion (see Higham et al., 2008).

Note that our model does not consider the hyperinflation of the mantle that often occurs during escape jets (Gosline et al., 1983; Thompson and Kier, 2001). Because hyperinflation of the mantle increases muscle fibre length before contraction, strain is likely to be even greater during escape jets.

Why do the SMR fibres have long thick filaments?

The muscular mantle wall of an adult *D. pealeii* can be over 5 mm thick, yet the combined cross-sectional area of the two SMR fibre layers represents only 4–6% of the total cross section of the mantle wall. Therefore, the loads experienced by the SMR fibres during hovering and slow jetting must be high, particularly because the CMP fibres are likely quiescent during these behaviours (Bartol, 2001a). Longer thick filaments (Josephson, 1975; Kier and Curtin, 2002) provide a means to increase the stress generated by the SMR fibres.

During hovering and slow swimming, squids undulate or flap their fins to generate thrust while also using the pulsed jet. The fins of squids, including *D. pealeii*, originate on cartilages embedded within and supported by the mantle musculature, and the mantle muscle and connective tissue fibres must resist the loads generated by the fins (Kier, 1989). Because the SMR fibres alone appear to be electrically active during hovering and slow jetting (Bartol, 2001a), the SMR fibres must not only provide power for jetting but also, in combination with mantle connective tissues, maintain mantle wall stiffness to support the fins. As highlighted by Mommsen and colleagues (Mommsen et al., 1981), the location of the two layers of the SMR fibres on the inner and outer surfaces of the mantle is ideal for pressurizing the entire mantle. Perhaps the longer thick filaments and corresponding higher P_0 of the SMR fibres are as important for maintaining mantle wall stiffness for fin support as for generating jet thrust at low swimming speeds. In this context, it is interesting that the timing of an ontogenetic increase in the thick filament length of the SMR fibres in the loliginid squid *Sepioteuthis lessoniana* coincides with a dramatic ontogenetic increase in the relative size of the fins (Thompson and Kier, 2006) (J. T. Thompson, unpublished observations).

Muscle specialization in squids

The use of mitochondria-rich fibres for slow swimming may be common in cephalopod muscle fibres. Small bundles of them are found in the transverse muscles of the fins of the Caribbean reef squid *Sepioteuthis sepioidea* and the European cuttlefish *Sepia officinalis* (Kier, 1989). Simultaneous recordings of electromyography and fin kinematics in *S. officinalis* suggested that the mitochondria-rich transverse fibres were used for continuous, low-amplitude fin movements while the mitochondria-poor fibres were recruited during higher amplitude fin beating (Kier et al., 1989).

Different circular muscle fibre types may not, however, be found in the mantles of all squids. A single type of circular muscle fibre with a small core of mitochondria, resembling the CMP fibres, is present in the mantles of many of the gelatinous-bodied mesopelagic and bathypelagic species (J. T. Thompson, in preparation). The majority of these animals rely primarily on fins for locomotion (Vecchione and Roper, 1991; Vecchione et al., 2002) and thus the factors that favored the evolution of CMP and SMR circular muscle fibres may not apply for these animals.

Mapping the distribution of the two circular muscle fibre types onto recent coleoid cephalopod phylogenies (Young and Vecchione, 1996; Carlini et al., 2000; Akasaki et al., 2006) suggests that the SMR/CMP distinction arose independently in several families of squids (J. T. Thompson, in preparation). Thus, study of the SMR and CMP circular muscle fibres of the mantle may provide an excellent opportunity to examine not only muscle mechanics but also the evolution of specialization in an obliquely striated muscle.

APPENDIX

Simple mantle model

(1) Solve for mantle wall thickness for a given decrease in diameter of the outer edge of the mantle [i.e. for a given amount of mantle contraction (MacGillivray et al., 1999)]:

$$t_f = r_f - \sqrt{r_f^2 - t_i(2r_i - t_i)}\ , \qquad \text{(A1)}$$

where t_i is the initial (i.e. resting) mantle wall thickness, t_f is the final wall thickness (i.e. at the end of contraction during the exhalant phase of the jet), r_i is the initial radius of the outer edge of the mantle, and r_f is the final radius of the outer edge of the mantle (see Fig. 9). Eqn 1 assumes that the length of the mantle does not increase during the jet (see Ward, 1972) and that the volume of the mantle tissue is constant.

(2) Calculate the circumferential strain (ε_{out}) at the outer edge of the mantle wall:

$$\varepsilon_{out} = -(2\pi r_i - 2\pi r_f) / 2\pi r_i\ . \qquad \text{(A2)}$$

This can be simplified to:

$$\varepsilon_{out} = -(r_i - r_f) / r_i\ . \qquad \text{(A3)}$$

The negative sign is arbitrary and indicates a decrease in mantle circumference.

(3) Calculate the circumferential strain (ε_{in}) at the inner edge of the mantle wall:

$$\varepsilon_{in} = -[(r_i - t_i) - (r_f - t_f)] / (r_i - t_i) . \quad (A4)$$

(4) Calculate the strain rate at the inner and outer edges by dividing the strain by the period of the exhalant phase of the jet. This approach provides the average strain rate over the period of the jet. Instantaneous strain rates may be higher.

(5) The magnitude of the transmural differences in strain is sensitive to the ratio r_i:t_i, with ε_{in} increasing as r_i:t_i decreases. In other words, the greater the relative thickness of the mantle wall, the greater the transmural difference in strain and strain rate.

(6) Increasing the length of the mantle during the jet (Packard and Trueman, 1974) has a minimal effect on the differences in transmural strain and strain rate. We calculated the volume (v) of the mantle tissue as:

$$v = \pi(r_{out}^2 - r_{in}^2)L , \quad (A5)$$

where r_{out} is the radius of the outer edge of the mantle, r_{in} is the radius of the inner edge of the mantle, and L is the length. Because the difference ($r_{out}^2 - r_{in}^2$) is proportional to the square of the thickness of the mantle wall (t), Eqn A5 can be rewritten as:

$$v \propto t^2 L . \quad (A6)$$

Solving for t and assuming the mantle is constant in volume (Ward, 1972) gives:

$$t \propto \sqrt{1 / L} . \quad (A7)$$

A 5% increase in mantle length (i.e. L=1.05) during mantle contraction yields an increase in mantle wall thickness that is only about 2.5% less than it would have been with no increase in mantle length.

(7) The transmural differences in strain and strain rate predicted by this model should apply to any cylindrical animal that has circumferentially arranged muscle fibres and an internal body cavity.

LIST OF ABBREVIATIONS

CMP	centrally located, mitochondria-poor
DML	dorsal mantle length
EMG	electromyographic
L_0	length
pcs	physiological cross section
P_0	peak tetanic force
SMR	superficially located, mitochondria-rich
SR	sarcoplasmic reticulum
T_{50}	50% peak
T_L	latent period
T_P	time to peak
Tw:Tt	twitch:tetanus ratio
v	volume
V	*in vivo* shortening velocity
V_{max}	maximum unloaded shortening velocity
ε	strain
$\dot{\varepsilon}$	strain rate

We are indebted to Dr Kevin J. Eckelbarger, director of the Darling Marine Center, for providing guidance and free use of the EM facility and supplies. We thank the staff of the Darling Marine Center, especially Mr Tim Miller and Ms Linda Healy, for help in finding and housing squid, and also for lab space and housing for ourselves. We also thank Ms Lisa Crescenti for assistance with estimating physiological cross section of the preparations. We thank anonymous reviewers of an earlier version of this manuscript and Dr William M. Kier for valuable suggestions. The research was supported by National Science Foundation grant IOS-0446081 to J.T.T., start-up funds from Franklin & Marshall College, and an Addison E. Verrill Marine Biology Fellowship from the Darling Marine Center to J.A.S.

REFERENCES

Akasaki, T., Nikaido, M., Tsuchiya, K., Segawa, S., Hasegawa, M. and Okada, N. (2006). Extensive mitochondrial gene arrangements in coleoid Cephalopoda and their phylogenetic implications. *Mol. Phylogenet. Evol.* **38**, 648-658.

Alexander, R. M. (1968). The orientation of muscle fibres in the myomeres of fishes. *J. Mar. Biol. Assoc. U. K.* **49**, 263-290.

Anderson, E. J. and DeMont, E. (2000). The mechanics of locomotion in the squid *Loligo pealei*: locomotory function and unsteady hydrodynamics of the jet and intramantle pressure. *J. Exp. Biol.* **203**, 2851-2863.

Bartol, I. K. (2001a). Role of aerobic and anaerobic circular mantle muscle fibers in swimming squid: electromyography. *Biol. Bull.* **204**, 59-66.

Bartol, I. K. (2001b). Swimming mechanics and behavior of the shallow-water brief squid *Lolliguncula brevis*. *J. Exp. Biol.* **201**, 3655-3682.

Bone, Q. and Ryan, K. P. (1974). On the structure and innervation of the muscle bands of *Doliolum* (Tunicata: Cyclomyaria). *Proc. R. Soc. Lond. B Biol. Sci.* **187**, 315-327.

Bone, Q., Pulsford, A. and Chubb, A. D. (1981). Squid mantle muscle. *J. Mar. Biol. Assoc. U. K.* **61**, 327-342.

Bone, Q., Packard, A. P. and Pulsford, A. L. (1982). Cholinergic innervation of muscle fibres in squid. *J. Mar. Biol. Assoc. U. K.* **62**, 193-199.

Bone, Q., Brown, E. R. and Usher, M. (1995). The structure and physiology of cephalopod muscle fibres. In *Cephalopod Neurobiology* (ed. N. J. Abbott, R. Williamson and L. Maddock), pp. 89-101. New York: Oxford University Press.

Bouligand, Y. (1966). La disposition des myofilaments chez une annélide polychète. *J. Microsc. Paris* **5**, 305-322.

Bozzola, J. J. and Russell, L. D. (1992). *Electron Microscopy. Principles and Techniques for Biologists*. Boston: Jones and Bartlett.

Brainerd, E. L. and Azizi, E. (2005). Muscle fibre angle, segment bulging and architectural gear ratio in segmented musculature. *J. Exp. Biol.* **208**, 3249-3261.

Brown, E. R., Usher, M. L. and Bone, Q. (1991). Physiological properties of squid mantle muscle bundles. *J. Mar. Biol. Assoc. U. K.* **71**, 732-733.

Burkholder, T. J. and Lieber, R. L. (2001). Sarcomere length operating range of vertebrate muscles during movement. *J. Exp. Biol.* **204**, 1529-1536.

Carlini, D. B., Reece, K. S. and Graves, J. E. (2000). Actin gene family evolution and the phylogeny of coleoid cephalopods (Mollusca: Cephalopoda). *Mol. Biol. Evol.* **17**, 1353-1370.

Carnevali, M. D. C., Saita, A. and Fedrigo, A. (1986). An unusual Z-system in the obliquely striated muscles of crinoids: three-dimensional structure and computer simulations. *J. Muscle Res. Cell Motil.* **7**, 568-578.

Collins, T. F. T. and Tsutsui, I. (2003). Neurotransmitters of mantle and fin muscles in spear squid, *Loligo bleekeri*. *J. Mar. Biol. Assoc. U. K.* **83**, 857-860.

Curtin, N. A. and Edman, K. A. P. (1994). Force-velocity relation for frog muscle fibres: effects of moderate fatigue and of intracellular acidification. *J. Physiol. Lond.* **475**, 483-494.

Curtin, N. A. and Woledge, R. C. (1988). Power output and force-velocity relationship of live fibres from white myotomal muscle of the dogfish, *Scyliorhinus canicula*. *J. Exp. Biol.* **140**, 187-197.

DeEguileor, M. and Valvassori, R. (1977). Studies on the helical and paramyosinic muscles. VII. Fine structure of body wall muscles in *Sipunculus nudus*. *J. Submicrosc. Cytol.* **9**, 363-372.

D'Haese, J. and Carlhoff, D. (1987). Localisation and histochemical characterisation of myosin isoforms in earthworm body wall muscle. *J. Comp. Physiol.* **157**, 171-179.

Edman, K. A. P. (1979). The velocity of unloaded shortening and its relation to sarcomere length and isometric force in vertebrate muscle fibres. *J. Physiol.* **291**, 143-159.

Eisenberg, B. R. (1983). Quantitative ultrastructure of mammalian skeletal muscle. In *Handbook of Physiology, Section 10, Skeletal Muscle* (ed. L. D. Peachey), pp. 73-112. Bethesda, MD: American Physiological Society.

Gilly, W. F., Preuss, T. and McFarlane, M. B. (1996). All-or-none contraction and sodium channels in a subset of circular muscle fibres of squid mantle. *Biol. Bull.* **191**, 337-340.

Gosline, J. M., Steeves, J. D., Harman, A. D. and DeMont, M. E. (1983). Patterns of circular and radial mantle muscle activity in respiration and jetting of the squid *Loligo opalescens*. *J. Exp. Biol.* **104**, 97-109.

Hanson, J. and Lowy, J. (1957). Structure of smooth muscles. *Nature* **180**, 906-909.

Higham, T. E., Biewener, A. A. and Wakeling, J. M. (2008). Functional diversification within and between muscle synergists during locomotion. *Biol. Lett.* **4**, 41-44.

Josephson, R. K. (1975). Extensive and intensive factors determining the performance of striated muscle. *J. Exp. Zool.* **194**, 135-154.

Kawaguti, S. and Ikemoto, N. (1957). Electron microscopy of the smooth muscle of a cuttlefish, *Sepia esculenta*. *Biol. J. Okayama Univ.* **3**, 196-208.

Kendrick-Jones, J., Szentkiralyi, E. M. and Szent-Györgyi, A. G. (1976). Regulatory light chains in myosins. *J. Mol. Biol.* **104**, 747-775.

Kier, W. M. (1985). The musculature of squid arms and tentacles: ultrastructural evidence for functional differences. *J. Morphol.* **185**, 223-239.

Kier, W. M. (1989). The fin musculature of cuttlefish and squid (Mollusca, Cephalopoda): morphology and mechanics. *J. Zool. Lond.* **217**, 23-38.

Kier, W. M. and Curtin, N. A. (2002). Fast muscle in squid (*Loligo pealei*): contractile properties of a specialized muscle fibre type. *J. Exp. Biol.* **205**, 1907-1916.

Kier, W. M. and Schachat, F. H. (1992). Biochemical comparison of fast- and slow-contracting squid muscle. *J. Exp. Biol.* **168**, 41-56.

Kier, W. M. and Schachat, F. H. (2008). Muscle specialization in the squid motor system. *J. Exp. Biol.* **211**, 164-169.

Kier, W. M., Smith, K. K. and Miyan, J. A. (1989). Electromyography of the fin musculature of the cuttlefish *Sepia officinalis*. *J. Exp. Biol.* **143**, 17-31.

Konno, K. (1978). Two calcium regulation systems in squid (*Ommastrephes sloani pacificus*) muscle. Preparations of calcium-sensitive myosin and troponin-tropomyosin. *J. Biochem.* **84**, 1431-1440.

Kuga, H. and Matsuno, A. (1988). Ultrastructural investigations on the anterior adductor muscle of a brachipoda, *Lingula unguis*. *Cell Struct. Funct.* **13**, 271-279.

Lännergren, J., Lindblom, P. and Johansson, B. (1982). Contractile properties of two varieties of twitch fibres in *Xenopus laevis*. *Acta Physiol. Scand.* **114**, 523-535.
Lowy, J. and Hanson, J. (1962). Ultrastructure of invertebrate smooth muscles. *Physiol. Rev. Suppl.* **42**, 34-47.
Maccatrozzo, L., Caliaro, F., Toniolo, L., Patruno, M., Reggiani, C. and Mascarello, F. (2007). The sarcomeric myosin heavy chain gene family in the dog: analysis of isoform diversity and comparison with other mammalian species. *Genomics* **89**, 224-236.
MacGillivray, P. S., Anderson, E. J., Wright, G. M. and DeMont, M. E. (1999). Structure and mechanics of the squid mantle. *J. Exp. Biol.* **202**, 683-695.
MacRae, E. K. (1965). The fine structure of muscle in a marine turbellarian. *Z. Zellforsch. Mikrosk. Anat.* **68**, 348-362.
Marceau, F. (1905). Recherches sur la structure des muscles du manteau des Céphalopodes en rapport avec leur mode du contraction. *Trav. Lab. Soc. Sci. Arachon. Ann.* **8**, 48-65.
Marden, J. H., Fitzhugh, G. H. and Wolf, M. R. (1998). From molecules to mating success: integrative biology of muscle maturation in a dragonfly. *Am. Zool.* **38**, 528-544.
Matsuno, A. and Kuga, H. (1989). Ultrastructure of muscle cells in the adductor of the boring clam *Tridacna crocea*. *J. Morphol.* **200**, 247-253.
Matulef, K., Sirokmán, K., Perreault-Micale, C. and Szent-Györgyi, A. G. (1998). Amino-acid sequence of squid myosin heavy chain. *J. Muscle Res. Cell Motil.* **19**, 705-712.
McLister, J. D., Stevens, E. D. and Bogart, J. P. (1995). Comparative contractile dynamics of calling and locomotor muscles in three hylid frogs. *J. Exp. Biol.* **198**, 1527-1538.
Messenger, J. B. M., Nixon and Ryan, K. P. (1985). Magnesium chloride as an anesthetic for cephalopods. *Comp. Biochem. Physiol.* **82C**, 203-205.
Milligan, B. J., Curtin, N. A. and Bone, Q. (1997). Contractile properties of obliquely striated muscle from the mantle of squid (*Alloteuthis subulata*) and cuttlefish (*Sepia officinalis*). *J. Exp. Biol.* **200**, 2425-2436.
Millman, B. M. (1967). Mechanism of contraction in Molluscan muscle. *Am. Zool.* **7**, 583-591.
Mommsen, T. P., Ballantyne, J., MacDonald, D., Gosline, J. and Hochachka, P. W. (1981). Analogues of red and white muscle in squid mantle. *Proc. Natl. Acad. Sci. USA* **78**, 3274-3278.
Norenburg, J. L. and Roe, P. (1997). Observations on musculature in pelagic nemerteans and on pseudostriated muscle in nemerteans. *Hydrobiologia* **356**, 109-120.
O'Dor, R. K. (1988). The forces acting on swimming squid. *J. Exp. Biol.* **137**, 421-442.
Ojima, T., Ohta, T. and Nishira, K. (2001). Amino acid sequence of squid troponin C. *Comp. Biochem. Physiol.* **129B**, 787-796.
Otis, T. S. and Gilly, W. F. (1990). Jet-propelled escape in the squid *Loligo opalescens*: concerted control by giant and non-giant motor axon pathways. *Proc. Natl. Acad. Sci. USA* **87**, 2911-2915.
Packard, A. and Trueman, E. R. (1974). Muscular activity of the mantle of *Sepia* and *Loligo* (Cephalopoda) during respiratory movements and jetting, and its physiological interpretation. *J. Exp. Biol.* **61**, 411-419.
Page, S. G. and Huxley, H. E. (1963). Filament lengths in striated muscle. *J. Cell Biol.* **19**, 369-390.
Prosser, C. L. and Young, J. Z. (1937). Responses of muscles of the squid to repetitive stimulation of the giant nerve fibres. *Biol. Bull.* **73**, 237-241.
Preuss, T., Lebaric, Z. N. and Gilly, W. F. (1997). Post-hatching development of circular mantle muscles in the squid *Loligo opalescens*. *Biol. Bull.* **192**, 375-387.
Rogers, C. M., Nelson, L., Milligan, B. J. and Brown, E. R. (1997). Different excitation-contraction coupling mechanisms exist in squid, cuttlefish and octopod mantle muscle. *J. Exp. Biol.* **200**, 3033-3041.
Rome, L. C. and Sosnicki, A. A. (1990). The influence of temerature on mechanics of red muscle in carp. *J. Physiol.* **427**, 151-169.
Rome, L. C. and Sosnicki, A. A. (1991). Myofilament overlap in swimming carp. II. Sarcomere length changes during swimming. *Am. J. Physiol.* **260**, C289-C296.
Rosenbluth, J. (1965). Ultrastructural organization of obliquely striated muscle fibers in *Ascaris lumbricoides*. *J. Cell Biol.* **25**, 495-515.
Rosenbluth, J. (1968). Obliquely striated muscle. IV. Sarcoplasmic reticulum, contractile apparatus, and endomysium of the body muscle of a polychaete, *Glycera,* in relation to its speed. *J. Cell Biol.* **36**, 245-259.
Rowlerson, A. M. and Blackshaw, S. E. (1991). Fibre types in leech body wall muscle. *J. Exp. Biol.* **157**, 299-311.
Schiaffino, S. and Reggiani, C. (1996). Molecular diversity of myofibrillar proteins: gene regulation and functional significance. *Physiol. Rev.* **76**, 371-423.
Sosnicki, A. A., Loesser, K. E. and Rome, L. C. (1991). Myofilament overlap in swimming carp. 1. Myofilament lengths of red and white muscle. *Am. J. Physiol.* **260**, C283-C288.
Swank, D. M., Zhang, G. and Rome, L. C. (1997). Contraction kinetics of red muscle in scup: mechanism for variation in relaxation rate along the length of the fish. *J. Exp. Biol.* **200**, 1297-1307.
Sweeney, H. L., Kushmerick, M. J., Mabuchi, K., Sréter, F. A. and Gergely, J. (1988). Myosin alkali light chain and heavy chain variations correlate with altered shortening velocity of isolated skeletal muscle fibers. *J. Biol. Chem.* **263**, 9034-9039.
Thompson, J. T. and Kier, W. M. (2001). Ontogenetic changes in fibrous connective tissue organization in the Oval Squid, *Sepioteuthis lessoniana* Lesson, 1830. *Biol. Bull.* **201**, 136-153.
Thompson, J. T. and Kier, W. M. (2006). Ontogeny of circular muscle ultrastructure and implications for jet locomotion in Oval Squid, *Sepioteuthis lessoniana*. *J. Exp. Biol.* **209**, 433-443.
Toniolo, L., Maccatrozzo, L., Patruno, M., Pavan, E., Caliaro, F., Rossi, R., Rinaldi, C., Canepari, M., Reggiani, C. and Mascarello, F. (2007). Fiber types in canine muscles: myosin isoform expression and functional characterization. *Am. J. Physiol.* **292**, C1915-C1926.
van Leeuwen, J. L., Lankheet, M. J. M., Akster, H. A. and Osse, J. W. M. (1990). Function of red axial muscles of carp (*Cyprinus carpio* L.): recruitment and normalized power output during swimming in different modes. *J. Zool. Lond.* **220**, 123-145.
Vecchione, M. and Roper, C. F. E. (1991). Cephalopods observed from submersibles in the western North Atlantic. *Bull. Mar. Sci.* **49**, 433-445.
Vecchione, M., Roper, C. E., Widder, E. A. and Frank, T. M. (2002). *In situ* observations on three species of large-finned deep-sea squids. *Bull. Mar. Sci.* **71**, 893-901.
Venable, J. H. and Coggeshall, R. (1965). A simplified lead citrate stain for use in electron microscopy. *J. Cell Biol.* **25**, 407-408.
Wakeling, J. M. and Johnston, I. A. (1999). White muscle strain in the common carp and red to white muscle gearing ratios in fish. *J. Exp. Biol.* **202**, 521-528.
Ward, D. V. (1972). Locomotory function of the squid mantle. *J. Zool. Lond.* **167**, 487-499.
Ward, S. M., McKerr, G. and Allen, J. M. (1986). Structure and ultrastructure of muscle systems within *Grillotia erinaceus* metacestodes (Cestoda, Trypanorhyncha). *Parasitology* **93**, 587-597.
Williams, L. W. (1909). *The Anatomy of the Common Squid Loligo pealii, Lesueur.* Leiden, Holland: E. J. Brill.
Young, I. S. and Rome, L. C. (2001). Mutually exclusive muscle designs: the power output of the locomotory and sonic muscles of the oyster toadfish (*Opsanus tau*). *Proc. R. Soc. Lond. B Biol. Sci.* **268**, 1965-1970.
Young, J. Z. (1938). The functioning of the giant nerve fibres of the squid. *J. Exp. Biol.* **15**, 170-185.
Young, R. E. and Vecchione, M. (1996). Analysis of morphology to determine primary sister-taxon relationships within coleoid cephalopods. *Am. Malacol. Bull.* **12**, 91-112.